

## Branching Ratio Measurement of the decay $K_L \rightarrow e^+e^-\mu^+\mu^-$ .

A. Alavi-Harati<sup>12</sup>, T. Alexopoulos<sup>12</sup>, M. Arenton<sup>11</sup>, K. Arisaka<sup>2</sup>, S. Averitte<sup>10</sup>, R.F. Barbosa<sup>7,\*\*</sup>, A.R. Barker<sup>5</sup>, M.Barrio<sup>4</sup>, L. Bellantoni<sup>7</sup>, A. Bellavance<sup>9</sup>, J. Belz<sup>10</sup>, R. Ben-David<sup>7</sup>, D.R. Bergman<sup>10</sup>, E. Blucher<sup>4</sup>, G.J. Bock<sup>7</sup>, C. Bown<sup>4</sup>, S. Bright<sup>4</sup>, E. Cheu<sup>1</sup>, S. Childress<sup>7</sup>, R. Coleman<sup>7</sup>, M.D. Corcoran<sup>9</sup>, G. Corti<sup>11</sup>, B. Cox<sup>11</sup>, M.B. Crisler<sup>7</sup>, A.R. Erwin<sup>12</sup>, R. Ford<sup>7</sup>, A. Glazov<sup>4</sup>, A. Golossanov<sup>11</sup>, G. Graham<sup>4</sup>, J. Graham<sup>4</sup>, K. Hagan<sup>11</sup>, E. Halkiadakis<sup>10</sup>, J. Hamm<sup>1</sup>, K. Hanagaki<sup>8</sup>, S. Hidaka<sup>8</sup>, Y.B. Hsiung<sup>7</sup>, V. Jejer<sup>11</sup>, D.A. Jensen<sup>7</sup>, R. Kessler<sup>4</sup>, H.G.E. Kobrak<sup>3</sup>, J. LaDue<sup>5</sup>, A. Lath<sup>10,†</sup>, A. Ledovsky<sup>11</sup>, P.L. McBride<sup>7</sup>, P. Mikelsons<sup>5</sup>, E. Monnier<sup>4,\*</sup>, T. Nakaya<sup>7</sup>, K.S. Nelson<sup>11</sup>, H. Nguyen<sup>7</sup>, V. O'Dell<sup>7</sup>, M. Pang<sup>7</sup>, R. Pordes<sup>7</sup>, V. Prasad<sup>4</sup>, B. Quinn<sup>4,§</sup>, X.R. Qi<sup>7</sup>, E.J. Ramberg<sup>7</sup>, R.E. Ray<sup>7</sup>, A. Roodman<sup>4</sup>, M. Sadamoto<sup>8</sup>, S. Schnetzer<sup>10</sup>, K. Senyo<sup>8</sup>, P. Shanahan<sup>7</sup>, P.S. Shawhan<sup>4</sup>, J. Shields<sup>11</sup>, W. Slater<sup>2</sup>, N. Solomey<sup>4</sup>, S.V. Somalwar<sup>10</sup>, R.L. Stone<sup>10</sup>, E.C. Swallow<sup>4,6</sup>, S.A. Taegar<sup>1</sup>, R.J. Tesarek<sup>10</sup>, G.B. Thomson<sup>10</sup>, P.A. Toale<sup>5</sup>, A. Tripathi<sup>2</sup>, R. Tschirhart<sup>7</sup>, S.E. Turner<sup>2</sup>, Y.W. Wah<sup>4</sup>, J. Wang<sup>1</sup>, H.B. White<sup>7</sup>, J. Whitmore<sup>7</sup>, B. Winstein<sup>4</sup>, R. Winston<sup>4</sup>, T. Yamanaka<sup>8</sup>, E.D. Zimmerman<sup>4</sup>

<sup>1</sup> University of Arizona, Tucson, Arizona 85721

<sup>2</sup> University of California at Los Angeles, Los Angeles, California 90095

<sup>3</sup> University of California at San Diego, La Jolla, California 92093

<sup>4</sup> The Enrico Fermi Institute, The University of Chicago, Chicago, Illinois 60637

<sup>5</sup> University of Colorado, Boulder, Colorado 80309

<sup>6</sup> Elmhurst College, Elmhurst, Illinois 60126

<sup>7</sup> Fermi National Accelerator Laboratory, Batavia, Illinois 60510

<sup>8</sup> Osaka University, Toyonaka, Osaka 560-0043 Japan

<sup>9</sup> Rice University, Houston, Texas 77005

<sup>10</sup> Rutgers University, Piscataway, New Jersey 08854

<sup>11</sup> The Department of Physics and Institute of Nuclear and Particle Physics, University of Virginia, Charlottesville, Virginia 22901

<sup>12</sup> University of Wisconsin, Madison, Wisconsin 53706

† To whom correspondence should be addressed.

\* Permanent address C.P.P. Marseille/C.N.R.S., France

\*\*Permanent address University of São Paulo, São Paulo, Brazil

## The KTeV Collaboration

### Abstract

We have collected a 43 event sample of the decay  $K_L \rightarrow e^+e^-\mu^+\mu^-$  with negligible backgrounds and measured its branching ratio to be  $(2.62 \pm 0.40 \pm 0.17) \times 10^{-9}$ . We see no evidence for CP violation in this decay. In addition, we set the 90% confidence upper limit on the combined branching ratios for the lepton flavor violating decays  $K_L \rightarrow e^\pm e^\pm \mu^\mp \mu^\mp$  at  $\mathcal{B}(K_L \rightarrow e^\pm e^\pm \mu^\mp \mu^\mp) \leq 1.23 \times 10^{-10}$ , assuming a uniform phase space distribution.

PACS numbers: 13.85.Rm, 13.25.Es, 14.40.Aq, 14.80.Ly

Typeset using REVTeX

We present the observation of the decay  $K_L \rightarrow e^+e^-\mu^+\mu^-$  and a measurement of its branching ratio. This decay proceeds entirely through the  $K\gamma^*\gamma^*$  vertex and provides the best opportunity for its study. Knowledge of the  $K\gamma^*\gamma^*$  vertex is crucial in order to extract short distance information, including the CKM matrix element  $V_{td}$ , from  $K_L \rightarrow \mu^+\mu^-$  decays. We are also able to search for CP violating effects in  $K_L \rightarrow e^+e^-\mu^+\mu^-$ , as well as the lepton-flavor violating decay  $K_L \rightarrow e^\pm e^\pm \mu^\mp \mu^\mp$ . The previous E799-I experiment measured  $\mathcal{B}(K_L \rightarrow e^+e^-\mu^+\mu^-) = (2.9_{-2.4}^{+6.7}) \times 10^{-9}$  [1] with one event.

There are several predictions for the branching ratio. Quigg and Jackson [2] have used a Vector Meson Dominance (VMD) model to predict a value of  $2.37 \times 10^{-9}$ . A phase-space model with both CP conserving and CP violating form factors by Uy [3] predicts values from  $(1.63 \pm 0.07) \times 10^{-9}$  for a totally CP conserving decay, to  $(3.67 \pm 0.15) \times 10^{-6}$  for a totally CP violating decay. Note that the CP violating form factors increase the branching ratio by over three orders of magnitude. This calculation does not take into account any momentum dependence of the form factors. An  $\mathcal{O}(p^6)$  Chiral Perturbation Theory calculation by Zhang and Goity [4] predicts  $(1.30 \pm 0.15) \times 10^{-9}$ .

The measurement presented here was performed as part of the KTeV experiment, which has been described elsewhere [5]. The data used were collected during the 1997 run. The KTeV experiment, as configured for rare decay searches (E799-II), used two nearly parallel kaon beams created by 800 GeV/c protons incident on a BeO target. The kaon decays used in our studies were collected in a decay region approximately 65 m long, situated 94 m from the production target.

Charged particles were detected by four drift chambers, each consisting of one horizontal and one vertical pair of planes, with typical resolution of 100  $\mu m$  per plane. Two drift chambers were situated on either side of an analysis magnet which imparted approximately 205 MeV/c of transverse momentum to the charged tracks. The drift chambers were followed by a trigger hodoscope bank and a 1.9 m  $\times$  1.9 m calorimeter composed of 3100 blocks of pure CsI. The fiducial volume was surrounded by a photon veto system used to reject events

in which photons missed the calorimeter. The calorimeter was followed by a muon filter composed of a 10 cm thick lead wall and three steel walls totalling 511 cm. The first plane of scintillators used to identify muons (MU2) was located after 400 cm of steel, behind the second steel wall. Two additional 3 m  $\times$  3 m scintillator planes (MU3Y and MU3X), located after the third steel wall and consisting of one horizontal and one vertical plane, defined the acceptance for muons. All muon scintillator planes had 15 cm segmentation.

The trigger for the signal events required hits in the upstream drift chambers consistent with at least two tracks, as well as two hits in the trigger hodoscopes. The calorimeter was required to have at least one cluster with over 1 GeV of energy, deposited within a 20 ns window relative to the event trigger. The muon counters MU3X and MU3Y were each required to have at least two hits. In addition, a preliminary online identification of  $K_L \rightarrow e^+e^-\mu^+\mu^-$  decays required a minimum of three tracks originating from a loosely defined vertex. A separate trigger was used to collect  $K_L \rightarrow \pi^+\pi^-\pi^0$  decays with subsequent Dalitz decays  $\pi^0 \rightarrow e^+e^-\gamma$  ( $K_L \rightarrow \pi^+\pi^-\pi_D^0$ ) which were used for normalization. This trigger was similar to the signal trigger but had no requirements on hits in the muon hodoscopes or clusters in the calorimeter. The preliminary online identification was performed on the normalization sample as well. The normalization mode trigger was prescaled by a factor of 500:1.

The offline analysis required four tracks from a single vertex. A cut on the vertex reconstruction  $\chi^2$  ensured the four tracks originated from the same vertex. Upstream and downstream track segments were allowed at most a 2 mm offset at the bend plane of the analysis magnet. The four track decay vertex projected to the calorimeter was required to be within one of the beam regions. A track was identified as  $e^\pm$  if it pointed to a cluster in the calorimeter with  $|E/P - 1| \leq 0.05$ , otherwise it was identified as a muon. The electromagnetic energy resolution of the calorimeter,  $\sigma(E)/E = 0.45\% \oplus 2.0\%/\sqrt{E}$  (GeV), was determined using a large sample of  $e^\pm$  from  $K_L \rightarrow \pi^\mp e^\pm \nu$  decays.

To remove muons which range out in the steel, events in which a muon track had

$P < 10$  GeV/c were discarded. To remove misidentified pions, events in which a muon track deposited over 3 GeV in the calorimeter were discarded. Events with excessive energy in the veto counters beyond that expected from accidental activity, or extra calorimeter clusters not associated with an electron or muon track, were also discarded.

A large component of the background consists of  $K_L \rightarrow \pi^+\pi^-\pi_D^0$  decays in which the charged pions simulate muons by punching through the muon filter or decaying in flight. A simulation of this background is compared to the data in figure 1. The invariant mass ( $M_{ee\mu\mu}$ ) distributions for the data and for the simulated background are shown after successful electron identification, but before cuts on vertex quality or extra calorimeter activity.

The events at high invariant mass are due to two kaons which decayed within the same Tevatron RF bucket (double decay events). An event with a double decay contains two separate two-track vertices, which usually form a poor four-track vertex. The vertex quality cut eliminated nearly all of the double decay events. The cuts on photon veto activity and extra calorimeter clusters removed 98% of the background from  $K_L \rightarrow \pi^+\pi^-\pi_D^0$ . Figure 1 also shows the data after the vertex quality and extra calorimeter clusters cut.

Another potentially large background comes from  $K_L \rightarrow \mu^+\mu^-\gamma$  events in which the gamma converts to an  $e^+e^-$  pair in the vacuum window. A cut requiring that either the two-electron invariant mass ( $M_{ee}$ ) be greater than 3 MeV/ $c^2$  or the separation for the two electron tracks at the first drift chamber be greater than 3 mm reduced the window conversion events by 98.8% while losing only 13.6% of the remaining signal events. We estimate a 0.19 event background from the vacuum window conversions.

The double decay background remaining after all cuts was estimated by examining events in which the two electrons were of the same charge sign. Two electrons (or two muons) that do not arise from the same decay have the same sign as often as opposite signs. Figure 2 shows scatter plots of  $M_{ee\mu\mu}$  vs.  $P_t^2$ , where  $P_t^2$  is the square of the transverse momentum with respect to the trajectory from the production target to the decay vertex. Figure 2(a) contains signal events with all but  $M_{ee\mu\mu}$  and  $P_t^2$  cuts, while figure 2(b) shows

the distribution for events that pass the same cuts, except that the two electrons (and muons) are required to have the same sign. There are 30 such like-sign events in the region  $0.25 \leq M_{ee\mu\mu} \leq 0.75 \text{ GeV}/c^2$  and  $P_t^2 \leq 0.02(\text{ GeV}/c)^2$ . We assume that this background is evenly distributed, and estimate a 0.02 event double decay background within the signal region. The  $M_{ee\mu\mu}$  vs.  $P_t^2$  data distribution shown in figure 2(a) contains 43 events within the signal box given by  $0.48 \leq M_{ee\mu\mu} \leq 0.51 \text{ GeV}/c^2$  and  $P_t^2 \leq 0.00025 (\text{GeV}/c)^2$ .

The remaining background at masses below  $M_K$  is mainly from  $K_L \rightarrow \pi^+\pi^-\pi_D^0$  decays with charged pion decay or punchthrough. Figure 3 shows the fit of the data with all but the invariant mass cut to a scaled background simulation, from which we estimate a background of 0.03 events in the signal region. The total background in the signal region, from window conversions of  $K_L \rightarrow \mu^+\mu^-\gamma$  decays,  $K_L \rightarrow \pi^+\pi^-\pi_D^0$  decays in which the charged pions either decay in flight or punchthrough the filter steel, and double decay events is estimated to be 0.24 events.

The geometric acceptance of the detector for the signal mode, calculated using a Monte Carlo generator which employed the matrix element formulated by Uy [3], was 6.1%. Only CP conserving elements of the matrix element were used for the acceptance calculation.

In order to calculate the branching ratio, we use the  $K_L \rightarrow \pi^+\pi^-\pi_D^0$  decay for normalization. These events were selected by the minimum-bias, two-track trigger described above. The cuts applied to the normalization mode were as similar to the signal mode as possible, with a few separate cuts specific to this mode, including the requirement that the photon cluster in the calorimeter deposit at least 5 GeV of energy in the calorimeter and be  $\geq 3$  cm away from the beam holes. We also required that the invariant mass of the  $e^+e^-\gamma$  be within 10 MeV/ $c^2$  of the  $\pi^0$  mass, and its energy be between 15 and 85 GeV. We determined that  $(2.70 \pm 0.08) \times 10^{11}$   $K_L$  within an energy range of 20 to 220 GeV decayed between 90 and 160 meters from the target. The error in this value is dominated by the uncertainty in the measured branching ratios for  $K_L \rightarrow \pi^+\pi^-\pi^0$  and  $\pi^0 \rightarrow e^+e^-\gamma$  [6].

While similar in most respects to the signal trigger, the normalization mode trigger

lacked any muon requirements. One source of systematic uncertainty in the normalization involved the response of the muon steel and counters. We evaluated the hit efficiencies of the muon counters using high statistics samples of  $\mu^\pm$  taken in runs with special absorbers and magnet configurations. The muon efficiency was  $\sim 99\%$  and nearly uniform across the counter planes. This efficiency was measured to  $\leq 0.5\%$  of itself. We used similar runs to study our scattering simulation. By selecting tracks which traversed an overlap of adjacent muon counters in MU2, we were able to determine the track position at the counter plane independent of the tracking system, and ensure the accuracy of the muon scattering simulation for incident muon momenta well below the 10 GeV/c cutoff.

We estimated the systematic uncertainty in the branching ratio due to any disagreements between the simulation and data by varying the selection cuts. The contribution due to uncertainties in the selection criteria for both the signal and normalization modes is 3%. Accidental activity in the detector caused a 3.7% uncertainty in the acceptance, while systematic uncertainty due to muon scattering in the lead and steel downstream of the calorimeter was estimated to be 0.5%. The change in signal acceptance due to possible form-factors in the matrix element of the decay contributed 3%, while the uncertainty due to background events remaining in the signal region was estimated at 0.6%.

The total systematic uncertainty was 6.4%, to be compared to 15.2% statistical uncertainty. Our final result is thus  $\mathcal{B}(K_L \rightarrow e^+e^-\mu^+\mu^-) = (2.62 \pm 0.40 \pm 0.17) \times 10^{-9}$ , where the first error is statistical and the second is systematic.

Events with like-sign leptons are a signature of lepton flavor violation, and given that we found no like-signed lepton events in our sample, we put a limit on the process  $K_L \rightarrow e^\pm e^\pm \mu^\mp \mu^\mp$ . Using a flat phase-space generator, similar analysis requirements and signal region as that used for the  $e^+e^-\mu^+\mu^-$  analysis, we found that the geometric acceptance for like-sign lepton events was 7.3%. With zero events in the signal region, we find that the combined  $\mathcal{B}(K_L \rightarrow e^\pm e^\pm \mu^\mp \mu^\mp) \leq 1.23 \times 10^{-10}$  at the 90% confidence level.

Uy [3] has carried out a phase space calculation for  $K_L \rightarrow e^+e^-\mu^+\mu^-$ , including a

CP violating term in the decay. The form factors used had no  $q^2$  dependence and were labelled  $g_2$  for the CP even and  $h_2$  for the CP odd component. According to this model, the total measured branching ratio is sensitive to the CP violating term. We measure the ratio  $(g_2/h_2)^2 \leq 2.71 \times 10^{-4}$  with 90% confidence.

The angular distributions of the decay products are also a sensitive probe of CP violating effects. Define the angle  $\phi$  to be the angle between the plane containing the  $e^+e^-$  and that containing the  $\mu^+\mu^-$ . An asymmetry about zero in the distribution  $\sin 2\phi$  is unambiguous evidence for CP violation. We have observed such an asymmetry in the decay  $K_L \rightarrow \pi^+\pi^-e^+e^-$  [7]. For the decay  $K_L \rightarrow e^+e^-\mu^+\mu^-$ , 18 (25) events are in the positive (negative)  $\sin 2\phi$  direction, consistent with zero asymmetry.

In principle, the  $K_L \rightarrow e^+e^-\mu^+\mu^-$  decay is the best mode to investigate the possible  $K\gamma^*\gamma^*$  form factors because there are no exchange terms to complicate the theoretical understanding. However, the low statistics makes determination of the form factors difficult at present. Figure 4 shows the distributions for  $M_{ee}$  and  $M_{\mu\mu}$  for the 43 signal events, along with the shape expected from a simulation without any momentum dependence in the form factors. Although there may be a discrepancy between data and MC prediction in the  $M_{\mu\mu}$  distribution indicative of the presence of a form factor, the lack of statistics makes a firm conclusion difficult at this time.

We have measured the branching ratio for the decay  $K_L \rightarrow e^+e^-\mu^+\mu^-$  to be  $(2.62 \pm 0.40 \text{ (stat)} \pm 0.17 \text{ (sys)}) \times 10^{-9}$ . Note that the VMD model of Quigg and Jackson [2] which predicts  $2.37 \times 10^{-9}$  is in better agreement with our result than more recent predictions. We have placed an upper limit on the CP violating term of Uy [3], of  $(\frac{g_2}{h_2})^2 \leq 2.71 \times 10^{-4}$  at the 90% C.L, using the branching ratio. We have also searched for lepton flavor violation in like-sign lepton decays, and placed a limit  $\mathcal{B}(K_L \rightarrow e^\pm e^\pm \mu^\mp \mu^\mp) \leq 1.23 \times 10^{-10}$  at the 90% confidence level. The 1999 run of KTeV will soon yield a larger statistics sample of  $K_L \rightarrow e^+e^-\mu^+\mu^-$  decays. Studies of form factors in these decays should advance the understanding of the  $K\gamma^*\gamma^*$  vertex, thereby constraining one of the largest sources of uncertainty in the



determination of the CKM matrix element  $V_{td}$  from  $K_L \rightarrow \mu\mu$  decays. In addition, a CP violating contribution might be detected with a larger sample of  $K_L \rightarrow e^+e^-\mu^+\mu^-$  decays.

We gratefully acknowledge the support and effort of the Fermilab staff and the technical staffs of the participating institutions for their vital contributions. This work was supported in part by the U.S. Department of Energy, the National Science Foundation and the Ministry of Education and Science of Japan.

## REFERENCES

- [1] P. Gu *et al.*, Phys. Rev. Lett. **76**, 4312 (1996).
- [2] C. Quigg, J.D. Jackson, unpublished, LBL preprint UCRL-18487 (1968).
- [3] Z. Uy, Phys. Rev. **D43**, 802 (1991).
- [4] L. Zhang, J.L. Goity, Phys. Rev. **D57**, 7031 (1998).
- [5] A. Alavi-Harati *et al.* Phys. Rev. Lett. **83**, 922 (1999).
- [6] Particle Data Group, D.E. Groom *et al.* Eur. Phys. J. **C15**, 400, 515 (2000).
- [7] A. Alavi-Harati *et al.* Phys. Rev. Lett. **84**, 408 (2000).

FIGURES

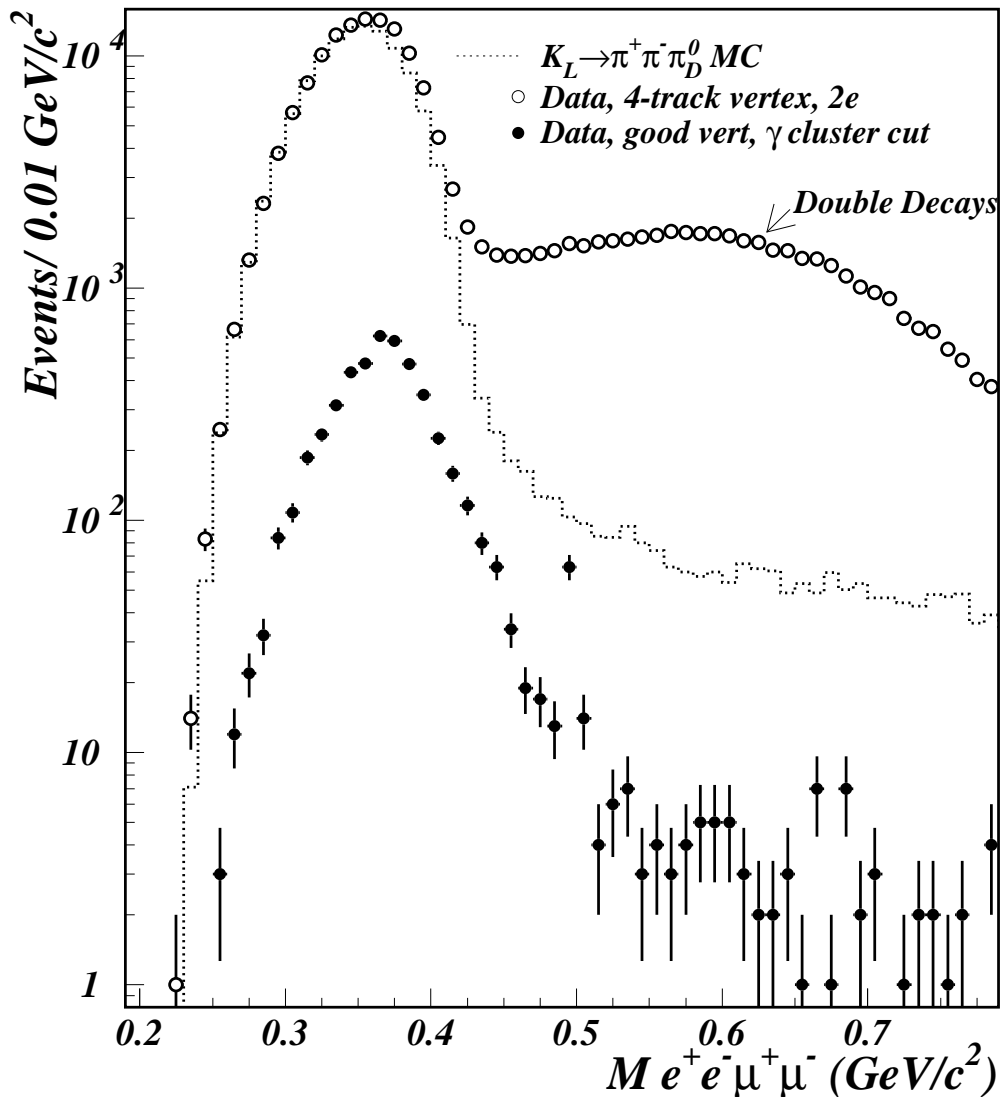


FIG. 1. Distribution of  $M_{ee\mu\mu}$  after finding a four-track vertex and identifying two of the tracks as  $e^\pm$  for data (hollow circles), and for Monte Carlo simulation of  $K_L \rightarrow \pi^+\pi^-\pi_D^0$  with charged pion punchthrough/decay at the same stage of analysis (dotted line). The simulation is normalized to the data below  $0.32 \text{ GeV}/c^2$ . The data distribution after cuts on vertex quality and any extra clusters in the calorimeter is shown by filled circles. A signal peak is visible at the kaon mass. At this stage of the analysis,  $\sim 20\%$  of the events in that peak are  $K_L \rightarrow \mu^+\mu^-\gamma$  with  $\gamma \rightarrow e^+e^-$  in the vacuum window.

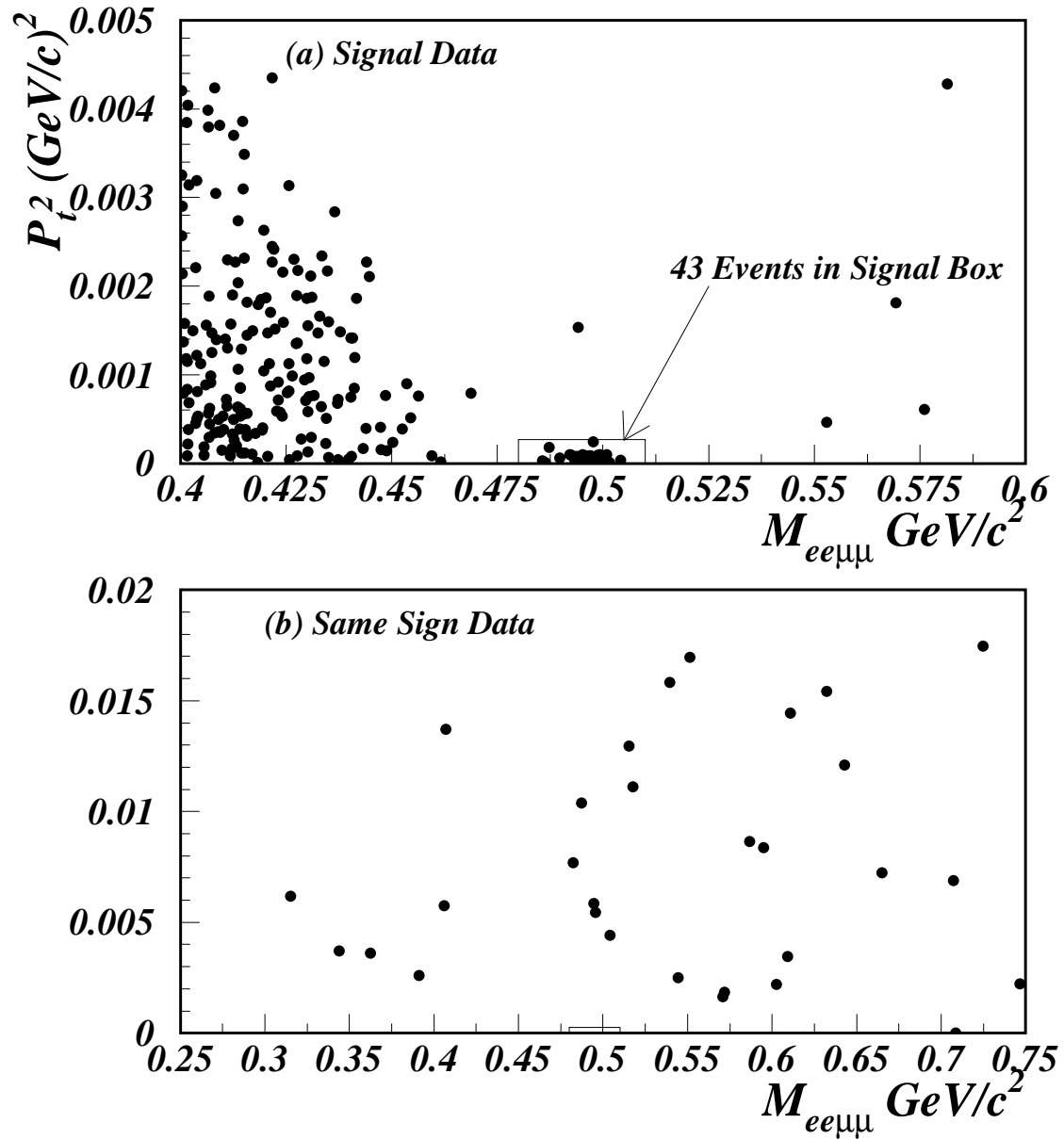


FIG. 2. Top plot (a) shows  $P_t^2$  vs.  $M_{ee\mu\mu}$  for  $K_L \rightarrow e^+e^-\mu^+\mu^-$ , signal events, with all cuts. There are 43 events in the signal box. Bottom plot (b) shows same sign lepton events,  $e^\pm e^\pm \mu^\mp \mu^\mp$ . There are no same sign events in the signal box. Note that the area in plot (b) is a factor of 10 larger than that in (a).

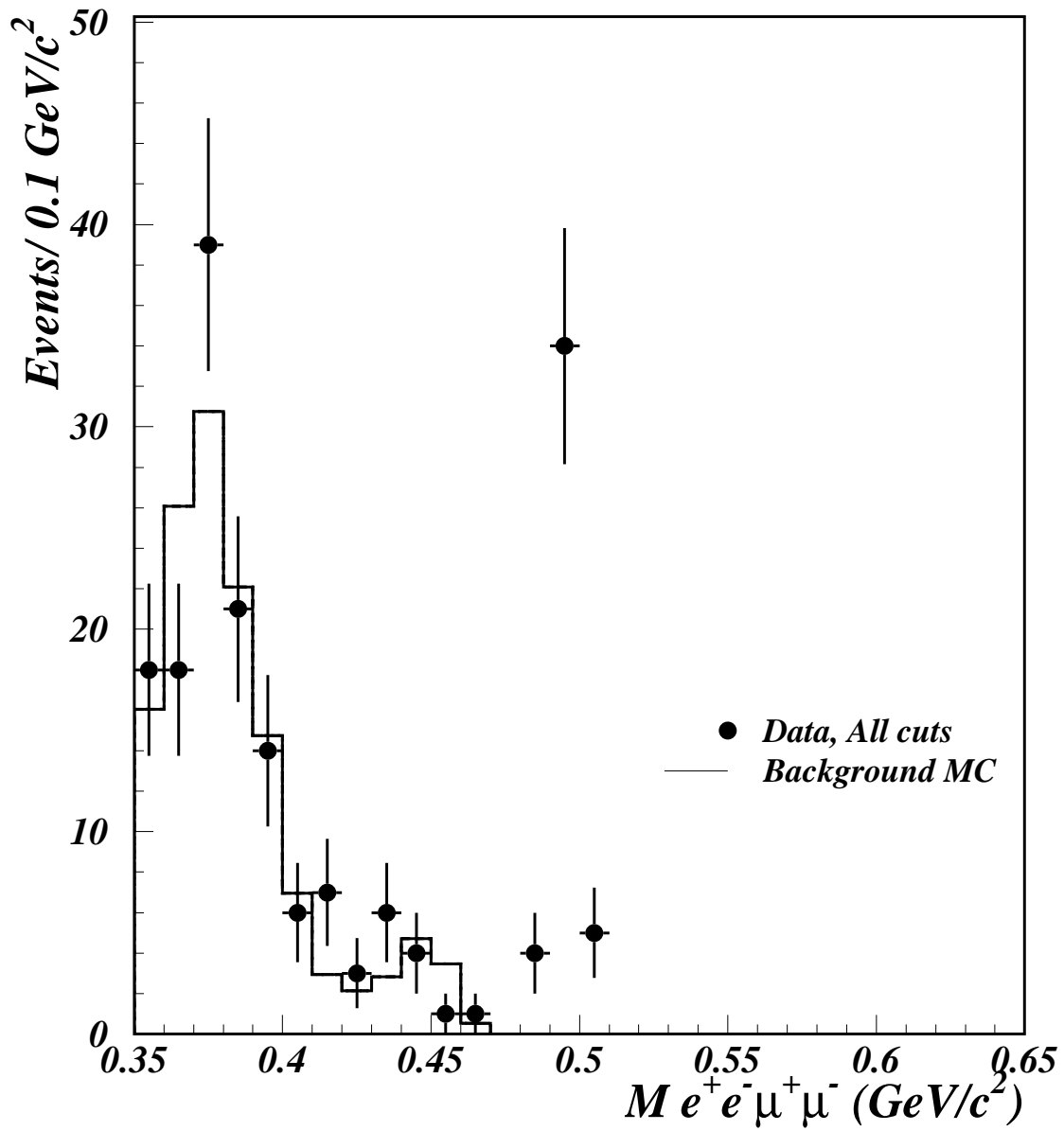


FIG. 3.  $M_{e\bar{e}\mu\bar{\mu}}$  for data (dots) and the scaled background simulation (line), with  $P_t^2 \leq 0.00025$   $(\text{GeV}/c)^2$ . The peak resolution for the signal is approximately  $4 \text{ MeV}/c^2$ .

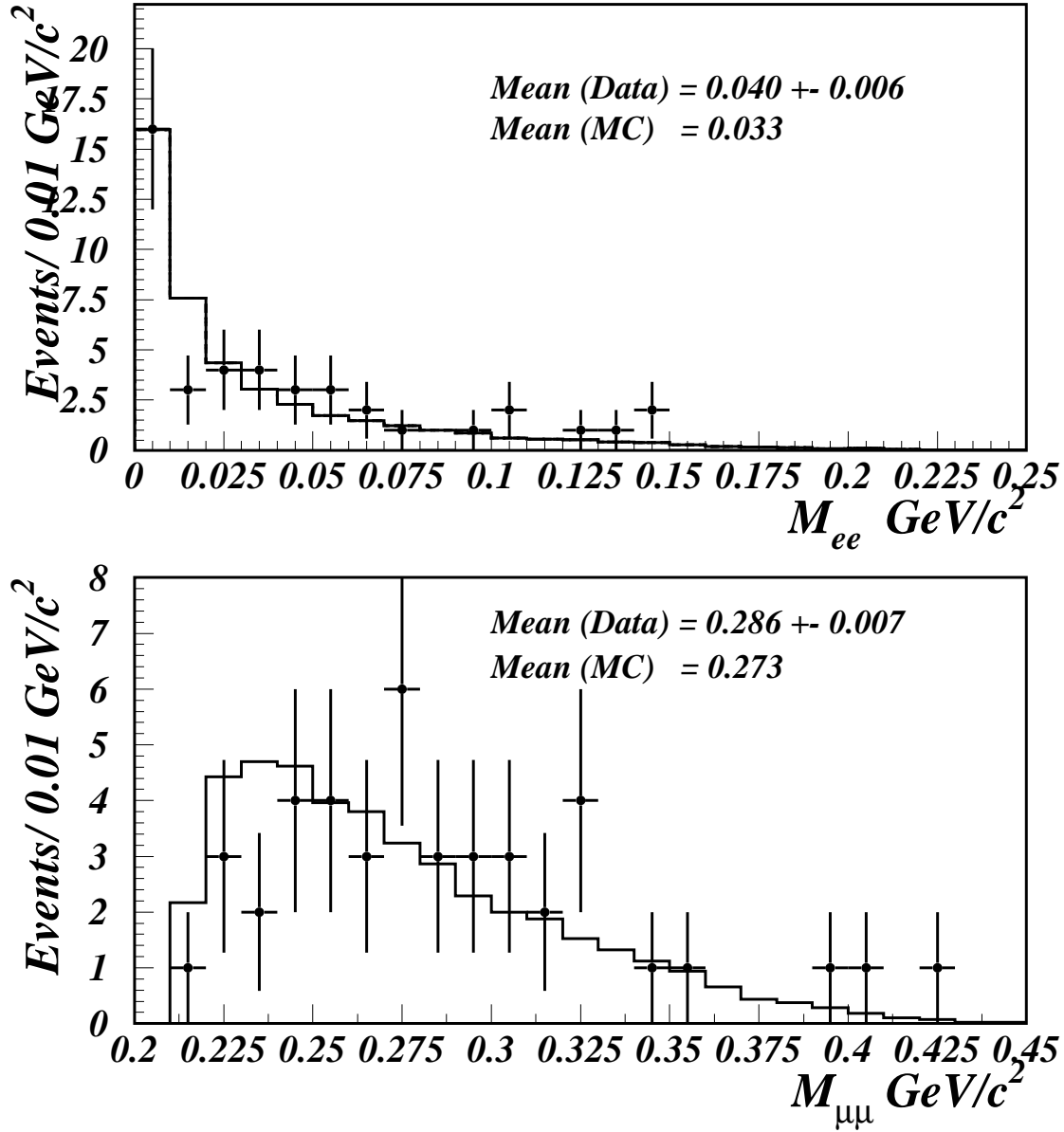


FIG. 4. The distributions of  $M_{ee}$  and  $M_{\mu\mu}$  for the 43 events observed in the data (dots) as well as that expected from a model without any momentum dependent form factors (line).